ACCOUNTS
of chemical research

Exploiting Peptide Nanostructures To Construct Functional Artificial Ion Channels

FRANÇOIS OTIS, MICHÈLE AUGER, AND NORMAND VOYER*

Département de Chimie and PROTEO, Faculté des Sciences et de Génie, Université Laval, Pavillon Alexandre-Vachon, 1045 avenue de la Médecine, Québec, Québec G1V 0A6, Canada

RECEIVED ON FEBRUARY 21, 2013

CONSPECTUS

Natural ion channel proteins possess remarkable properties that researchers could exploit to develop nanochemotherapeutics and diagnostic devices. Unfortunately, the poor stability, limited availability, and complexity of these structures have precluded their use in practical devices. One solution to these limitations is to develop simpler molecular systems through chemical synthesis that mimic the salient properties of artificial ion channels.

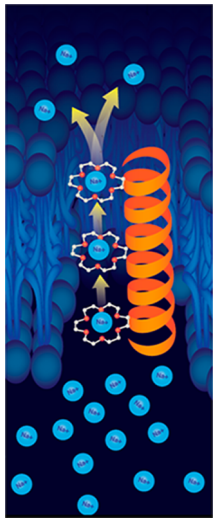

Inspired by natural channel proteins, our group has developed a family of peptide nanostructures thatcreate channels for ions by aligning crown ethers on top of each other when they adopt an α-helical conformation. Advantages to this crown ether/peptide framework approach include the ease of synthesis, the predictability of their conformations, and the ability to fine-tune and engineer their properties.

We have synthesized these structures using solid phase methods from artificial crown ether amino acids made from L-DOPA. Circular dichroism and FTIR spectroscopy studies in different media confirmed that the nanostructures adopt the predicted α-helical conformation. Fluorescence studies verified the crown ether stacking arrangement. We confirmed the channel activity by single-channel measurements using a modified patch-clamp technique, planar lipid bilayer (PLB) assays, and various vesicle experiments. From the results, we estimate that a 6 Å distance between two relays is ideal for sodium cation transport, but relatively efficient ion transport can still occur with an 11 Å distance between two crown ethers. Biophysical studies demonstrated that peptide channels operate as monomers in an equilibrium between adsorption at the surface and an active, transmembrane orientation.

Toward practical applications of these systems, we have prepared channel analogs that bear a biotin moiety, and we have used them as nanotransducers successfully to detect avidin. Analogs of channel peptide nanostructures showed cytotoxicity against breast and leukemia cancer cells.

Overall, we have prepared well-defined nanostructures with designed properties, demonstrated their transport abilities, and described their mechanism of action. We have also illustrated the advantages and the versatility of polypeptides for the construction of functional nanoscale artificial ion channels.

Introduction

Developing functional well-characterized artificial ion channels is of primary importance for the preparation of innovative nanochemotherapeutics and diagnostic devices. Although mimicking ion carriers was achieved with great success, designing synthetic structures mimicking the properties of ion channel proteins turned out to be a daunting task for chemists. The complexity of the structure and the ion transport mechanism of natural channel proteins have greatly increased the challenges for molecular designers. Nevertheless, elegant approaches have been reported that led to synthetic channels mimicking certain features of channel proteins.[1−6] However, incorporation of those artificial channels into functional devices is still an unmet challenge despite intense research efforts.[7] This is mainly due to synthetic hurdles and poorly defined mechanism of ion transport.

Inspired by natural ion channel proteins, we have been researching in this field for the past 20 years trying to exploit peptide helical structures as molecular frameworks to construct artificial channels that can operate as single species and not through aggregation. In the sections below, we review our approach and the most significant results obtained, as well as some drawbacks encountered along the way toward unimolecular peptide-based artificial ion channels.

Published on the Web 04/29/2013 www.pubs.acs.org/accounts
10.1021/ar400044k

Design Strategy

Many natural ion channel proteins create ion pores using specific arrangements of transmembrane α-helices.[8,9] Some artificial structures also exploited this characteristic. DeGrado and co-workers described a synthetic system in which α-helices can aggregate together and conduct protons across a membrane.[10] Inspired by such structures, we envisioned creating a family of ion channels by using the ability of α-helices to incorporate into and to span the nonpolar environment of a lipid bilayer membrane and adding to them elements that will be able to create a favorable environment where the ions could easily circulate.

We opted for the crown ethers, macrocyclic structures known for their capacity of binding cations.[11] Indeed, crown ethers possess several interesting features that make them attractive for channel formation.[12,13] They are neutral and generally poor ion binders with fast on−off rates.[14] Also, the synthetic methods to prepare crown ethers are well described. Finally, it is possible to fine-tune their ion binding properties by adjusting their diameter. By building a crown ether onto an amino acid, we can introduce them into an α-helix at strategic positions in such a way that they will be aligned on top of each other to create a channel for ions. The overall length of this structure has to be long enough to span a typical lipid bilayer, so we opted for a helix made from 21 amino acids.

There are numerous advantages to this crown ether/peptide framework approach. First, we have the possibility of accurately predicting the solution conformation of peptide structures from the primary structure to facilitate the design "on paper". Second, preparation of these structures can be easily achieved by peptide solid phase synthesis, which leads to the possibility of rapidly creating a large number of analogs incorporating different crown ethers for ion selectivity and the possibility of postsynthesis molecular engineering to incorporate selectively functional groups, linkers, recognition elements, etc. Third, the availability of efficient purification and characterization techniques (MS, HPLC) for peptides of that size offer additional tools to fully and easily characterize the new structures. Finally, we have access to a wide range of powerful biophysical techniques to study peptide structure, conformation, and assembly, affording us a detailed understanding of their mechanism of action and helping to shed light on complex ion channel proteins and facilitate their incorporation into practical devices.

Synthesis

The synthetic strategy has been based on a combination of solid phase peptide synthesis and solution synthesis. Macrocyclic amino acids were made in solution from fully protected L-3,4-dihydroxyphenylalanine (L-DOPA) and dibromo-oligo(ethylene glycol) derivatives leading to a variety of crown ether amino acids.[15,16] The acidic function was then deprotected, and the new building blocks were used in peptide synthesis using classical protocols. We first selected Kaiser resin with a *N*-*t*-butoxycarbonyl protection strategy to prepare heptapeptide segments from crown-ether amino acid derivatives and alanine, which were cleaved and condensed in solution.[17]

Although successful, the alanine-based peptides turned out to be plagued with very poor solubility in both polar and apolar media. To increase solubility, alanine has been replaced by leucine in the second generation of the model peptide and segment condensation was performed directly on the resin support with a final cleavage only at the end of the synthesis.[15] This strategy had the advantage of permitting a large diversity in N- and C-termini, because the cleavage was effected using various nucleophiles.[18] Segment condensations still remained problematic in certain cases. With the improvements in solid phase peptide synthesis protocols and reagents, we recently adopted a stepwise strategy using Wang resin and the 9-fluorenylmethyloxycarbonyl (Fmoc) protecting group to prepare new channel analogs. This led to improved yields and purity and the possibility of creating an almost limitless number of channel analogs introducing different natural or unnatural amino acids at any position within the sequence of interest.[16,19] The purity of all peptides was confirmed by analytical HPLC. Purification was performed on a semipreparative HPLC column. The peptide nanostructures were then characterized by mass spectrometry.

Figure 1 presents an overview of the crown peptides prepared with different chain lengths and sizes of macrocycle. Compounds **1**−**3** were made from 21-crown-7-derived L-phenylalanine with lengths of 21, 14, and 7 amino acids, protected with an *N*-*t*-butoxycarbonyl group at the N-terminus and a methyl ester at the C-terminus. The 7- and 14-mer were prepared to be used as controls in transport experiments. Other 21-mer peptides were made from 18-crown-6 (**4**), 15-crown-5 (**5**), 13-crown-4 (**6**), and 14-crown-4 (**7**) derivatives with same N- and C-termini. Figure 2 shows N- and C-termini variations on peptide **3**. In all cases, crown ether residues were incorporated at positions to be aligned when the peptide backbone adopts an α-helical conformation.

Analogs with different numbers of macrocycles were also prepared.[19] To avoid too-long domains of leucines that could affect the solubility and increase aggregation and to

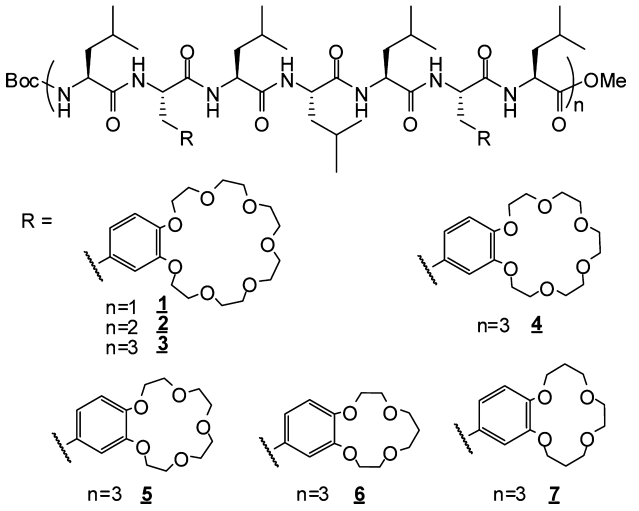

FIGURE 1. Peptide analogs with different sizes of crown ether and lengths.

keep the aromatic stacking effect stabilizing the conformation and alignment of crown ethers, we replaced L-leucine by L-alanine in the center of leucine triads and substituted crown ethers by phenylalanines (Figure 3). Both termini have been kept deprotected.

Conformational Analysis

On the basis of our design of a channel created by alignment of crown ethers, we had to confirm that the nanostructures that bear macrocycles were adopting an α-helical conformation in media where they should be operating. We thus have analyzed all crown peptides prepared first by circular dichroism spectroscopy (CD). Figure 4a (solid line) exhibits a typical CD spectrum for peptide **3**, characteristic of the spectra obtained for all the prepared nanostructures.[20] The spectrum indicates a clear preference for the predicted α-helical conformation, in which the macrocycle alignment can form a functional channel.

This conclusion is supported by FTIR spectroscopy studies, where only the absorption at 1657 cm^{-1}, characteristic of amide I band of α-helices, is observed.[21] Importantly, the helical conformation is conserved in different media, protic (TFE, MeOH) or hydrophobic (1,2-dichloroethane) (Figure 4a). Variations of peptide concentration in TFE did not lead to changes in ellipticity at 222 nm (Figure 4b), a strong indication that peptide **3** and its analogs do not tend to aggregate in low polarity environments.[20]

Helical conformation is also preserved in a typical model membrane: egg yolk phosphatidylcholine (EYPC) vesicles (Figure 4a, dashed and dotted line). CD studies showed that the partial decrease of the 208 nm band ellipticity can be associated with the orientation of the helical peptide in the

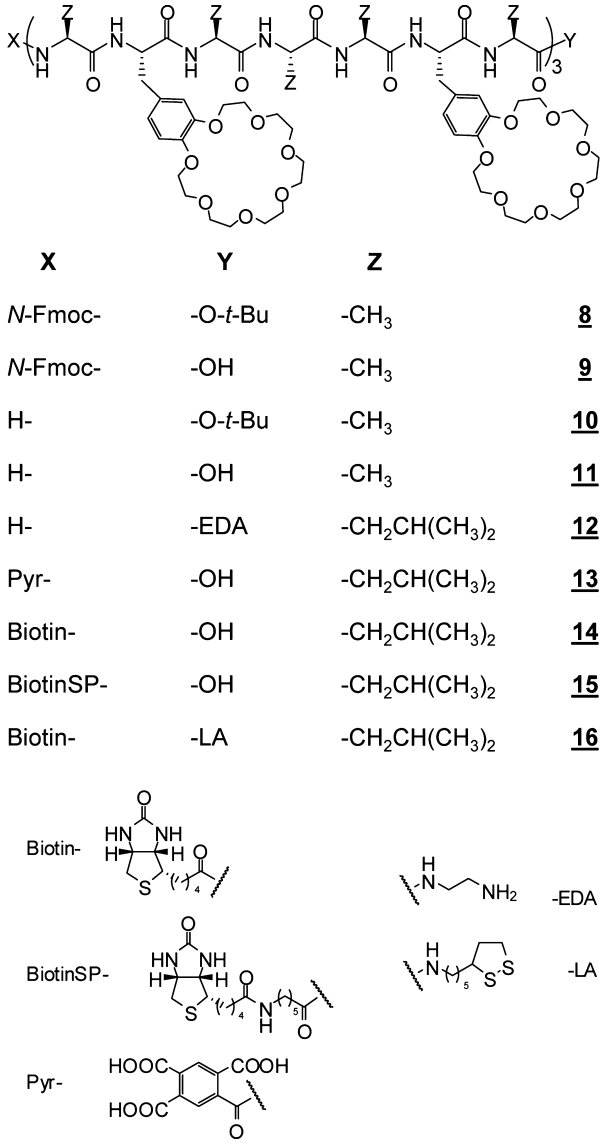

FIGURE 2. Peptide analogs with different N- and C-termini (SP, spacer from 6-aminohexanoic acid; Pyr, pyromellitic acid; EDA, ethylene diamine; LA, (±)-α-lipoic acid).

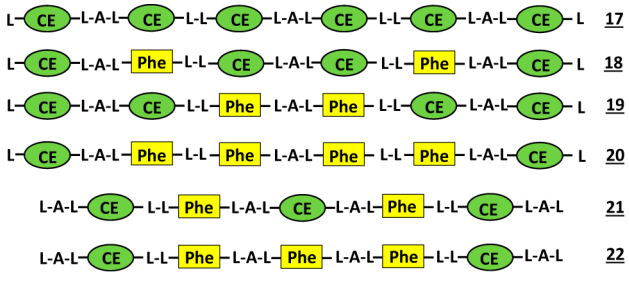

FIGURE 3. Peptide analogs containing different number of crown ethers. N- and C-termini are deprotected, CE stands for 21-C-7 phenylalanine derivative. Compounds **23**, **24**, and **25** are similar to **17** with CE being 18-C-6, 15-C-5, and 13-C-4, respectively.

bilayer on the quartz surface. It is known that the CD spectra of perpendicularly oriented α-helices exhibit a loss of this

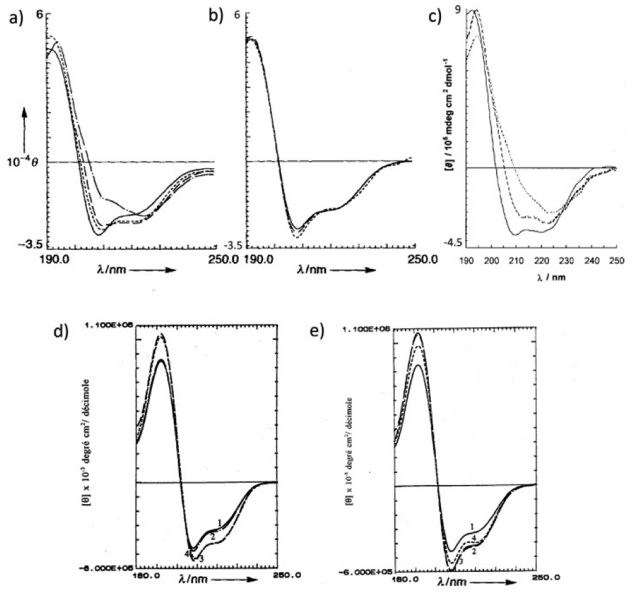

FIGURE 4. Circular dichroism spectra in mean residue molar ellipticity at 25 °C: (a) peptide **3** in 2,2,2-trifluoroethanol (TFE) (—), methanol (· · ·), 1,2-dichloroethane (– – –), and egg yolk lecithine (EYPC) vesicle (– · –); (b) peptide **3** in TFE at different concentrations, 2.3×10^{-4} M (—), 2.3×10^{-5} M (– – –), and 2.3×10^{-6} M (· · ·); (c) peptide **6** in solution (TFE) (—), in EYPC (80:1 lipid/peptide) with a 0.01 cm cell (· · ·), and in EYPC with a 0.05 cm cell (– – –); (d) peptide **3** in TFE in presence of water, 100% TFE (line 1), 10% H_2O (line 2), 25% H_2O (line 3), and 50% H_2O (line 4); (e) peptide **3** in TFE without ion (line 1), with Na^+ (line 2), with K^+ (line 3), and with Cs^+ (line 4). Reprinted with permission from John Wiley and Sons, refs 20 and 21, **Copyright 1997 and 2000.**

signal.[22] The cuvettes used for CD measurements have very small optical pathlengths that permit bilayer alignment on the quartz surface. Indeed, when longer optical pathlengths are used, the orientation is lost, and the intensity of the 208 nm band increases (Figure 4c).[21] Similarly, CD studies show that presence of water or metal ions do not affect the conformation of peptide **3** (Figure 4d,e).

The crown ether stacking arrangement has been further confirmed by studying the fluorescence behavior of **10** (Figure 5). Compared with the 21-crown-7 phenylalanine derivative, the intensity of the emission band of the peptide showed an important hypochromic effect with a quantum yield approximately half the size relative to the crown amino acid alone, while the maximum wavelength shifts from 335 nm for the crown ether to 320 nm. We attribute those phenomena to the stacking interactions between the spatially adjacent aromatic fluorophores, as observed in face-to-face stacked porphyrin molecules.[17]

Ion Transport Properties

In order to demonstrate the channel activity of our nanostructures, we carried out single-channel measurements on

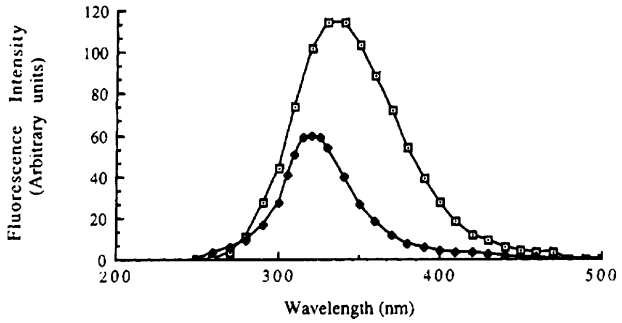

FIGURE 5. Fluorescence spectra of **10** (●) and the methyl ester of the 21-C-7 L-phenylalanine (□) at 25 °C in methanol. The λ_{max} observed are 320 and 335 nm, respectively. Reprinted with permission from ref 17. Copyright 1991 American Chemical Society.

3 using a modified patch-clamp technique.[23] In an initial investigation, K^+ transport was studied because this ion is weakly bound by 21-C-7 macrocycles, so potassium should traverse channels with great facility. In a typical experiment, a small amount of a solution of **3** in methanol was added to an unbuffered 1 M KCl solution (pH 5.8) in a 2 mL cell; the bilayer was constructed on a pipet from zwitterionic dipalmitoylphosphatidylcholine (DPPC) or uncharged glycerol monooleate (GMO). A transmembrane potential was applied, and the conductance was recorded. Results shown in Figure 6 are characteristic of ion channel activity observed with natural proteins.[20] We observed typical transitions between open and closed states; the discrete conductances are determined by the number of channels in the open state. A current of 3.5 pA with a 1 s lifetime was observed in the DPPC bilayer, while in GMO membranes, the current (1.0 pA) and lifetime (200 ms) were smaller.

Assays on planar lipid bilayer (PLB) were also performed with **8**–**11** to acquire more data on the channel activity of peptide nanostructures.[24] A bilayer was formed from a mixture of phosphatidylethanolamine and diphytanoylphosphatidylcholine (50/50) over a hole between two cuvettes filled with a NaCl buffered solution. A small aliquot of the peptide was then added from a DMSO stock solution. Current was measured using two electrodes disposed at each side of the membrane. The best results were obtained for **11**, the fully deprotected version of the channel. For **8**, the fully protected analog, and **9** and **10**, the C-and N-terminal deprotected channels, respectively, instability of channel incorporation in the membrane is observed, demonstrating the importance of polar and charged terminal groups for stabilizing the channel in a transmembrane, active orientation. Figure 7 shows typical membrane conductivity observed for **11** at positive and negative potentials with

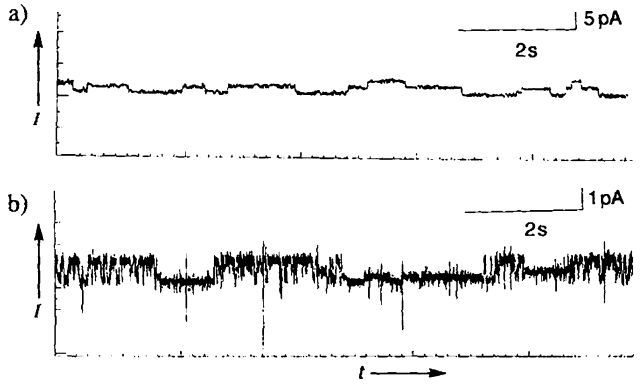

FIGURE 6. Single channel conductance recordings of peptide **3** in 1 M KCl (at +100 mV, filtered at 200 Hz) (a) in a DPPC bilayer (current level 3.5 pA, average lifetimes of open states >1 s) and (b) in GMO bilayer (current level 1.0 pA, average lifetimes of open states <200 ms). Reprinted with permission from John Wiley and Sons, ref 20, Copyright 1997.

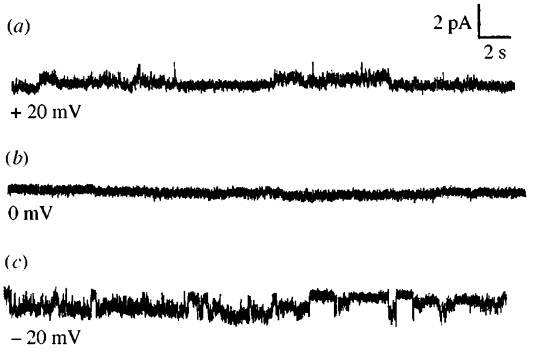

FIGURE 7. Typical membrane conductivity observed with **11** at positive (a) and at negative (c) potentials using symmetrical NaCl solutions (100 mM on both sides of the bilayer) and absence of unitary current at 0 mV (b). Reprinted with permission from the Royal Society of Chemistry, ref 24, Copyright 1997.

amplitudes in the range of 1−2 pA with variable open channel lifetimes. These results support the single channel activity of our structures for sodium transport and are in agreement with previous patch clamp data.[20]

In order to have a better understanding of the transport ability of our compounds and their mechanism of action, different vesicle assays were used.[19,25] One of them involves the preparation of unilamellar vesicles with an internal pH of 6.2 encapsulating a pH-dependent probe.[19] The dilution of these vesicles in an external solution with a large amount of NaCl and a pH of 7.2 creates opposite cation and proton gradients. Efficient channels allow cations to enter the vesicles while protons escape to preserve the ionic equilibrium, leading to the increase of internal pH, detected by changes in fluorescence. By establishing 100% transport ability as the maximal fluorescence obtained by destruction of vesicles with a surfactant, it is possible to compare the activity of many channels.

This method has the advantage of being simple and allowing a rapid screening of the transport ability of many analogs for different cations. We therefore used this technique to better understand the importance of the distance between the crown rings acting as ion relays by testing analogs with different numbers of crown ethers and also different distances between them. Figure 3 shows that the six analogs studied have six, four, three, or two macrocycles (21C7) with maximum distances between crown rings calculated to vary from 6 to 28 Å when a minimized helical conformation is adopted.

As presented in Table 1, the most efficient transport for sodium cations was achieved by channel structure **17**, which has six crown ethers separated by a maximum distance of 6 Å. Moderate transport ability was also observed for **18** and **21**, analogs that bear four and three crown rings, respectively, for the largest relay distance of 11 Å. But as soon as the distance between two crown ethers is over 11 Å, as for analogs **19**, **20**, and **22**, ion translocation is not significantly detected. This indicates that an interval of 17 Å and larger is too long to achieve efficient transport. Globally, results show that even if a 6 Å distance between two relays is ideal for sodium cation transport, a distance of 11 Å can be tolerated for relatively efficient channel activity. These results are in good agreement with results obtained from some natural ion channels, as for gramicidin A, which is known to possess two ion-relay sites separated by 11.6 Å.[26] It is important to mention that control experiments to detect vesicle lysis based on calcein release have been performed to ensure that the fluorescence increase detected in all vesicle studies was really due to ion transport and not due to membrane lysis or perturbation effects.[19]

The same assay was used to probe the ion selectivity of the crown channels and to prove that ions travel through the channel made from the crown ether stacks and not through undefined pores formed by peptide aggregates. We therefore synthesized hexacrown peptide analogs of **17** with artificial amino acids modified with different crown ether sizes (18C6, 15C5, and 13C4). Results are shown in Table 2.

We observed that Cs^+ was easily transported by **17**, the channel formed with 21C7. However, the transport ability decreased dramatically with analog bearing 18C6 (**23**) and was very low or not observed for smaller crowns. This could be explain by the large radius of Cs^+ (169 pm), which may have difficulties passing through crown ethers smaller than 21C7, which has a pore radius of ~170 pm.[27] The very low

TABLE 1. Percentage of Sodium Cation Transport at 400 s and Maximum Relay Distance for Peptides Bearing Six, Four, Three, or Two Crown Ethers

compound	no. of crown ethers	maximum distance (Å)	% transport
17	6	6	43
18	4	11	14
21	3	11	16
19	4	17	2
22	2	22	6
20	2	28	7

TABLE 2. Percentage of Cation Transport at 400 s Observed with Hexacrown Peptide Channels Having Crown Ethers of Different Diameters

		% transport			
compound	crown ether	Li^+	Na^+	K^+	Cs^+
17	21C7	31	33	53	62
23	18C6	17	28	38	13
24	15C5	16	12	7	8
25	13C4	10	2	2	2

transport of Cs^+ by **23**–**25** could also be due to nonspecific hoping along the crown peptides. In comparison, K^+, with a radius of 133 pm, translocated through 21C7 and 18C6 with good efficiency, the pore radius of 134–143 pm of 18C6 being large enough for K^+ flux. The 86–92 pm cavity of 15C5 does not lead to significant potassium transport. For the even smaller 13C4, potassium transport was also negligible. Na^+, with a radius of 95 pm, did pass through analogs bearing 15C5 **24** and larger crown ethers (**23**, **17**), but the smaller diameter of 13C4 (55–70 pm) precluded any transport.[28] Finally, for Li^+, which has a radius of 68 pm, transport was noticeable for all channels, with even a modest but significant transport activity for **25**, bearing 13C4. These results strongly support a channel mechanism where ions pass through the crown ether stack, as ion transport via an aggregated pore would not lead to the observed selectivity. Additionally, these results open the door to the development of highly functionalized nanoscale devices based on ion-selective artificial channels.

Membrane Incorporation and Orientation

In order to confirm our hypothesis of a transport mechanism that implies a transmembrane orientation of the peptides, we recorded polarized infrared attenuated total reflectance (ATR) spectra of an oriented dimyristoylphosphatidylcholine (DMPC) membrane in the absence and presence of the nanostructures. In a typical experiment, a DMPC membrane was formed on a germanium crystal by covering it with a lipid solution (either with or without the peptide), then completely evaporating the solvent. The lipid orientation

TABLE 3. ATR Studies of Crown Peptides **3** in DMPC Bilayers at Different Lipid/Peptide Molar Ratios[a]

	spectral bands			
	ν_{C-H} sym		ν_{amidel}	
sample	*R*	θ	*R*	θ
DMPC	1.09	25.5		
3 (10:1)	1.26	33.5	1.86	58.1
3 (20:1)	1.24	32.5	1.73	61.8
3 (40:1)	1.24	32.6	1.77	60.8
3 (60:1)	1.22	31.7	1.92	56.7

[a]Reprinted with permission from John Wiley and Sons, ref 21, Copyright 2000.

was calculated from the transition moment of the symmetric CH_2 stretching mode, which is assumed to be uniformly distributed with an angle of 90° with the axis of the lipid chain. For the peptide, the angle between the stretching vibration of the carbonyl (amide I) and the axis of an α-helix is fixed at 35°.[21] By acquiring spectra with infrared radiation polarized parallel or perpendicular to the germanium crystal, we can determine a dichroic ratio, from which the mean angle between the lipid or peptide axis and the bilayer normal can be found. The orientation of peptide **3** was investigated as a function of the molar lipid/peptide ratio.[21] Table 3 presents the results.

Information collected from the dichroic ratio of the CH_2 groups of pure DMPC indicated that the orientation of the lipid chains (25.5°) is in good agreement with those described by other groups.[29] In systems that include peptide **3**, the orientation of lipid molecules is slightly different, with an average orientation of the acyl chain between 31.7° and 33.5°.

As well, it should be noted that this change of orientation can be interpreted as a broadening of the orientation distribution. We can however conclude that incorporation of peptide induces a change at the level of the acyl chains of lipids. Regarding the orientation of peptide, the average orientation of helices ranged from 56.7° to 61.8°, with dichroic ratios from 1.73 to 1.92.

Three interpretations can be made from these results. First, a value of 2.0 could derive from a randomly oriented peptide and could indicate the presence of peptide aggregation. However, the fact that the dichroic ratio tends to diverge away from 2.0 at a 20:1 lipid/peptide ratio demonstrates that the orientation angles observed at this concentration are significant. Hence, the aggregation is not significant.

Second, we can interpret the results by assuming that the peptide is really oriented between angles of 57° to 62° in the lipid bilayer. However, the change in the value of angles as a

function of the molar ratio makes this hypothesis improbable, because the value would be the same independent of the molar ratio.

Finally, these orientation angles may originate from an average between two orientations of the peptide in the presence of a membrane: one at 90°, where the peptide is adsorbed at the surface of the bilayer, and another at 30°, where the peptide is in a transmembrane position, parallel to the lipid chains. This hypothesis could also explain the gating effect observed in single channel measurements, where an open state and a closed state were detected (see the Ion Transport Properties section). On the basis of this model, we can estimate the proportion of each orientation from the dichroic ratio *R*, knowing that an *R* value of 1.3 describes an orientation of 90°. An *R* value of 3.6 describes an orientation of 30°. Results at a molar ratio of 10:1 indicate that about 27% of the peptide is incorporated at 30°, while the remaining is adsorbed at 90°. Results for similar peptide nanostructures with different crown ether sizes or terminal groups are similar to those obtained with **3**.[21]

To validate the above hypothesis, we turned to solid state NMR spectroscopy (ssNMR), a powerful method to study peptide–membrane interactions.[30] Peptide **3** was used for ^{31}P and ^{2}H ssNMR experiments in the presence of DMPC or DMPG (dimyristoylphosphatidylglycerol) vesicles at lipid/peptide ratios of 60:1 and 20:1 (Figure 8).[31] Results from the ^{31}P experiments showed that the dynamics or the orientation of the polar phosphate groups or both are significantly affected by the presence of **3**. In addition, the same experiment using bicelles as a model membrane indicated that **3** has a negligeable impact on the morphology and orientation of the bicelles. Together, these results support the previous conclusion that in absence of a driving force, most of the peptide **3** prefers to be adsorbed at the surface of the bilayer. Interestingly, studies demonstrated that **3** interacts more strongly with the neutral DMPC bilayer than with the negatively charged DMPG bilayer. This could indicate that crown peptide nanostructures such as **3** interact preferably with eukaryotic cell membranes, compared with prokaryotic cell membranes.

To further pinpoint the interactions of **3** with bilayers, we turned to ssNMR using bilayers oriented between stacked glass plates.[32] An ^{15}N NMR experiment with a labeled analog of **3** and DMPC bilayers revealed that the peptide sits predominantly at the surface in agreement with previous results. Analyzing the ^{13}CO spinning sidebands of **3** also supports its predominant surface orientation.

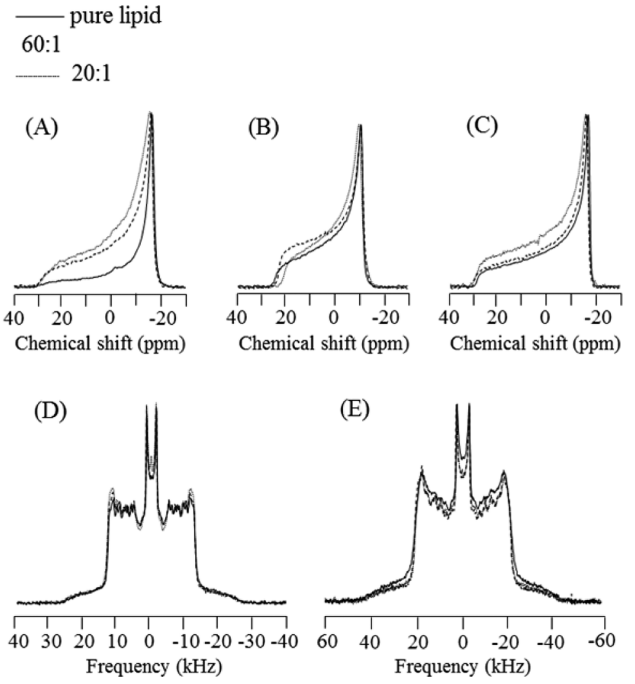

FIGURE 8. ^{31}P NMR spectra of (A) zwitterionic DMPC, (B) anionic DMPG, and (C) zwitterionic DMPC/cholesterol membranes at 37 °C in the absence and presence of the 21-mer peptide. ^{2}H NMR spectra of zwitterionic (D) DMPC and (E) DMPC/cholesterol membranes at 37 °C in the absence and presence of **3**. Reprinted with permission from Elsevier, ref 31, Copyright 2006.

All of our biophysical studies confirm that the crown peptide channels operate as monomers that are in an orientation equilibrium, existing mainly adsorbed at the surface of the bilayer membrane and with a significantly lower number of structures in a transmembrane, active orientation. The equilibrium could be responsible for the gating mechanism of such channel structures. The active orientation will be favored when a driving force is applied to the bilayer due to the intrinsic macrodipole of peptide helical structures.

Postsynthesis Engineering and Potential Applications

In order to render these nanostructures useful for practical applications, we explored various avenues to modify N- and C-termini to introduce connectors and recognition elements. Several groups have demonstrated the potential of gold nanoparticles[33,34] and gold surfaces[35] for molecular sensing. With the purpose of exploiting such functional systems, we added a disulfide group, derived from lipoic acid, to the C-terminal of peptide **3**. This disulfide function is known to anchor polypeptide efficiently to gold.[36]

We attached a biotin at the N-terminal position to act as a recognition element to exploit the biotin–avidin system in

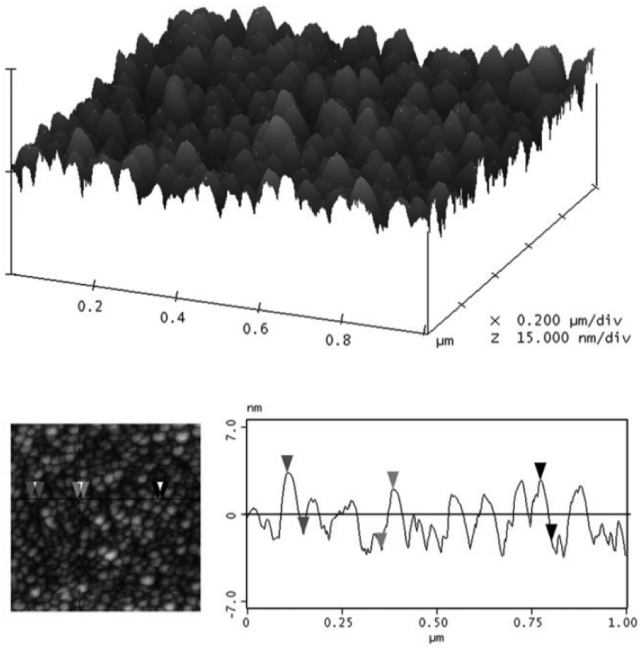

FIGURE 9. (top) Surface plot of a gold surface functionalized with peptide nanostructure **16** and (bottom) top view of SAM of peptide **16** (left) and a typical section analysis of the peptide clusters showing regular heights between 5 and 6 nm (right). Reprinted with permission from the Royal Society of Chemistry, ref 16, Copyright 2007.

model studies.[37] Using the new peptide channel **16**, we demonstrated the possibility of preparing gold nanoparticles and self-assembled monolayers on gold surfaces.[16] Figure 9 shows the peptide/gold monolayers observed by atomic force microscopy (AFM), showing the presence of cylindrical clusters of peptide with diameters varying from 20 to 60 nm and heights from 5 to 6 nm on average. These data fit very well with the estimated dimension of 5.3 nm for peptide **16**. We also confirmed that the peptide framework retains its α-helical conformation when adsorbed on gold (data not shown). These results illustrate the possibility of using crown peptide nanostructures coupled to electroactive substrates in sensitive detection assays.

To prove that the blockage of the channel could serve in detecting biologically relevant molecules, we studied a vesicle assay that takes advantage of the sensitivity of fluorescence spectroscopy. Using vesicles with encapsulated pyranine, a pH-sensitive fluorescent probe, we detected the presence of avidin with biotin-derived channel peptides **14** and **15**. Figure 10 shows that addition of avidin to those peptides significantly decreases the percentage of sodium transported, suggesting that avidin binds to the biotin probe, altering ion transport by blocking the channel entrance or extracting the channel from the membrane.[38] Controls with channel **3** that lack biotin or use a nonspecific protein (BSA)

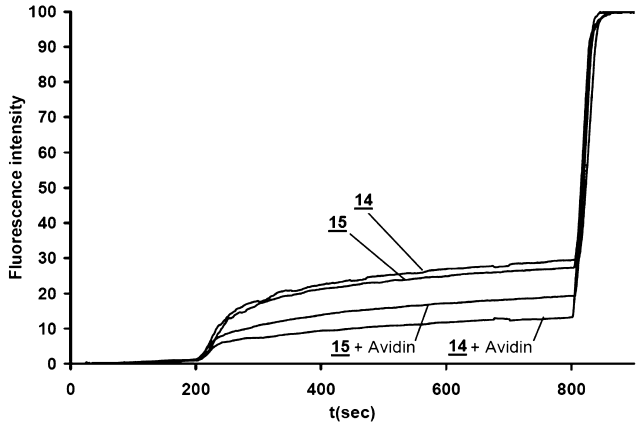

FIGURE 10. Change of fluorescence induced by addition of **14** and **15** with and without avidin. Peptides were added at 200 s and a surfactant (Triton X-100) allowed the destruction of all vesicles at 800 s to determine the maximum fluorescence.[38]

support the implication of a specific biotin–avidin interaction in the changes observed in fluorescence. We are presently extending the assay to the detection of carbohydrate ligands by different proteins, some of which are known to be overexpressed at the surface of some types of cancer cells,[39] in the perspective of developing new diagnostic tools.

Nanochemotherapeutics

Because crown channel nanostructures are designed to be active on biological membranes, bioactivity of several analogs has been investigated, especially antimicrobial activity and cytotoxicity.[15] We tested peptide 21-mer **3** on several bacteria, both Gram positive and Gram negative, but no antimicrobial activity could be found. The charged nature of the membrane of bacteria could probably explain these results and incorporation of cationic amino acids within the primary sequences should improve the antimicrobial potential of the artificial channels.

However, channel peptides **3** and **5** showed cytotoxic activities against breast cancer cells (MDA) and mouse leukemia cells (P388), while **1**, the truncated channel (heptamer version of the peptide), and the monomeric crown ether (21C7) were totally inactive (Table 4). These results confirm the importance of the crown peptides having an appropriate length (nanoscale) to span the membrane to exhibit cytotoxicity. The deprotected versions of **3** with charged head groups (**12** and **13**) are less active than **3** itself and were found to be not easily incorporated in bilayer membranes. Nevertheless, activities found for **3** and **5** are currently being optimized and engineered to be selective to cancer cells in order to avoid undesired hemolytic side effects. Toward this objective, we already have demonstrated the possibility

TABLE 4. Cytotoxicity of Different Peptide Nanostructures on Cancer Cells[a]

compound	MDA LD_{50} (μM)	P388 LD_{50} (μM)
Boc-7mer-OMe (21C7), **1**	*b*	35.0
Boc-21mer-OMe (21C7), **3**	15.0	8.5
Boc-21mer-OMe (15C5), **5**	10.0	2.5
Boc-21C7-OMe	*b*	*b*
H-21mer-EDA (21C7), **12**	15.0	*b*
Pyr-21mer-OH (21C7), **13**	>30.0	>40.0

[a]Reprinted with permission from Elsevier, ref 15, Copyright 2004. [b]Not determined due to low toxicity.

of fine-tuning membrane incorporation, and therefore cytotoxicity, by engineering N- and C-termini with short peptide sequences.[40] Work along these lines is being actively pursued.

Conclusions

We have demonstrated the advantages and the versatility of polypeptides to construct functional, well-defined nanostructures with designed man-made properties. The preparation of a family of peptide nanostructures that can act as functional artificial ion channels is a nice illustration of the strong potential of the approach. It should be re-emphasized that the powerful synthetic methods of peptide synthesis allow the rapid preparation of large unimolecular weight compounds in the nanoscale dimension. Likewise, a plethora of state-of-the-art biophysical techniques can be used to gain a detailed understanding of the structure, conformation, and mechanism of peptide-based devices. It is foreseeable that many other peptide nanostructures could be developed to perform a wide range of tasks.

The work described was performed using grants from the NSERC of Canada, the FRQNT, and the Université Laval. We are indebted to all the students, postdoctoral scholars, and research assistants that contributed to the work described. We also thank Pierre Audet for help in performing some NMR spectroscopy experiments.

BIOGRAPHICAL INFORMATION

François Otis was born in Matane, Québec, Canada. He received his B.Sc. in Chemistry in 2000 and an M.Sc. in Chemistry in 2003 from the Université Laval. He is currently working as research professional in the group of Normand Voyer, dedicating his laboratory efforts to bioorganic and supramolecular chemistry projects.

Michèle Auger is Professor of Chemistry at Université Laval in Québec City, Canada. She received her Ph.D. in Chemistry in 1990 under the direction of Ian C.P. Smith at the University of Ottawa and the National Research Council of Canada, and she did her postdoctoral work in the laboratory of Robert G. Griffin at the Massachusetts Institute of Technology in 1990−1991. Her current research efforts are focused on the solid-state NMR study of antimicrobial and amyloid peptides, silk proteins, and protein−lipid interactions in model membranes.

Normand Voyer was born in St-Eustache, Quebec, Canada. He earned his B.Sc. in Chemistry from the Université Laval and obtained his Ph.D. in Organic Chemistry also from Laval. After postdoctoral research with D. J. Cram at UCLA and with W. F. DeGrado at E. I. DuPont De Nemours & Co., he started his academic career at the Université de Sherbrooke in 1988 establishing research projects on the development of functional peptide nanostructures. He returned to Laval in 1996 where he is Professor of Bioorganic Chemistry and Director of the Quebec Research Network on Protein Function, Structure and Engineering, PROTEO.

FOOTNOTES

*To whom correspondence should be addressed. Phone: (+1)418-656-3613. Fax: (+1)418-656-7916. E-mail: normand.voyer@chm.ulaval.ca.
The authors declare no competing financial interest.

REFERENCES

1 Moszynski, J. M.; Fyles, T. M. Mechanism of ion transport by fluorescent oligoester channels. *J. Am. Chem. Soc.* **2012**, *134*, 15937–15945.
2 Gokel, G. W.; Negin, S. Synthetic membrane active amphiphiles. *Adv. Drug Delivery Rev.* **2012**, *64*, 784–796.
3 Matile, S.; Jentzsch, A. V.; Montenegro, J.; Fin, A. Recent synthetic transport systems. *Chem. Soc. Rev.* **2011**, *40*, 2453–2474.
4 Grosse, W.; Essen, L. O.; Koert, U. Strategies and perspectives in ion-channel engineering. *ChemBioChem* **2011**, *12*, 830–839.
5 Davis, J. T.; Okunola, O.; Quesada, R. Recent advances in the transmembrane transport of anions. *Chem. Soc. Rev.* **2010**, *39*, 3843–3862.
6 Satake, A.; Yamamura, M.; Oda, M.; Kobuke, Y. Transmembrane nanopores from porphyrin supramolecules. *J. Am. Chem. Soc.* **2008**, *130*, 6314–6315.
7 Takeuchi, T.; Matile, S. Sensing applications of synthetic transport systems. *Chem. Commun.* **2013**, *49*, 19–29.
8 Sheppard, D. N.; Welsh, M. J. Structure and function of the CFTR chloride channel. *Physiol. Rev.* **1999**, *79*, S23–S45.
9 Doyle, D. A.; Cabral, J. M.; Pfuetzner, R. A.; Kuo, A. L.; Gulbis, J. M.; Cohen, S. L.; Chait, B. T.; MacKinnon, R. The structure of the potassium channel: Molecular basis of K+ conduction and selectivity. *Science* **1998**, *280*, 69–77.
10 Lear, J. D.; Wasserman, Z. R.; DeGrado, W. F. Synthetic amphiphilic peptide models for protein ion channels. *Science* **1988**, *240*, 1177–1181.
11 Pedersen, C. J. The discovery of crown ethers (Nobel Lecture). *Angew. Chem., Int. Ed.* **1988**, *27*, 1021–1027.
12 Gokel, G. W.; Leevy, W. M.; Weber, M. E. Crown ethers: Sensors for ions and molecular scaffolds for materials and biological models. *Chem. Rev.* **2004**, *104*, 2723–2750.
13 Wright, K.; Anddad, R.; Lohier, J. F.; Steinmetz, V.; Wakselman, M.; Mazaleyrat, J. P.; Formaggio, F.; Peggion, C.; De Zotti, M.; Keiderling, T. A.; Huang, R.; Toniolo, C. Synthesis, ion complexation study, and 3D-structural analysis of peptides based on crown-carrier, C(alpha)-methyl-L-DOPA amino acids. *Eur. J. Org. Chem.* **2008**, 1224–1241.
14 Fyles, T. M. Electrostatic ion binding by synthetic receptors. In *Cation Binding by Macrocycles*; Gokel, G. W., Inoue, Y., Eds.; Dekker: New York, 1990; pp 203−251.
15 Biron, E.; Otis, F.; Meillon, J. C.; Robitaille, M.; Lamothe, J.; Van Hove, P.; Cormier, M. E.; Voyer, N. Design, synthesis, and characterization of peptide nanostructures having ion channel activity. *Bioorg. Med. Chem.* **2004**, *12*, 1279–1290.
16 Boutin, J. M.; Richer, J.; Tremblay, M.; Bissonette, V.; Voyer, N. Synthesis and characterization of peptide nanostructures chemisorbed on gold. *New J. Chem.* **2007**, *31*, 741–747.
17 Voyer, N. Preparation of supramolecular devices using peptide-synthesis - Design and synthesis of a tubular hexacrown molecule. *J. Am. Chem. Soc.* **1991**, *113*, 1818–1821.
18 Voyer, N.; Lavoie, A.; Pinette, M.; Bernier, J. A convenient solid-phase preparation of peptide substituted amides. *Tetrahedron Lett.* **1994**, *35*, 355–358.
19 Otis, F.; Racine-Berthiaume, C.; Voyer, N. How far can a sodium ion travel within a lipid bilayer? *J. Am. Chem. Soc.* **2011**, *133*, 6481–6483.
20 Meillon, J. C.; Voyer, N. A synthetic transmembrane channel active in lipid bilayers. *Angew. Chem., Int. Ed.* **1997**, *36*, 967–969.

21 Biron, E.; Voyer, N.; Meillon, J. C.; Cormier, M. E.; Auger, M. Conformational and orientation studies of artificial ion channels incorporated into lipid bilayers. *Biopolymers* **2000**, *55*, 364–372.

22 Olah, G. A.; Huang, H. W. Circular-dichroism of oriented alpha-helices. 1. Proof of the exciton theory. *J. Chem. Phys.* **1988**, *89*, 2531–2538.

23 Woolley, G. A.; Jaikaran, A. S. I.; Zhang, Z. H.; Peng, S. Y. Design of regulated ion channels using measurements of cis-trans isomerization in single molecules. *J. Am. Chem. Soc.* **1995**, *117*, 4448–4454.

24 Voyer, N.; Potvin, L.; Rousseau, E. Electrical activity of artificial ion channels incorporated into planar lipid bilayers. *J. Chem. Soc., Perkin Trans. 2* **1997**, 1469–1471.

25 Voyer, N.; Robitaille, M. A novel functional artificial ion-channel. *J. Am. Chem. Soc.* **1995**, *117*, 6599–6600.

26 Wallace, B. A. Recent advances in the high resolution structures of bacterial channels: Gramicidin A. *J. Struct. Biol.* **1998**, *121*, 123–141.

27 Steed, J. W.; Atwood, J. L. *Supramolecular chemistry*; John Wiley & Sons: Chichester, U.K., 2000.

28 Ulewicz, M.; Walkowiak, W.; Bartsch, R. A. Ion flotation of zinc(II) and cadmium(II) with proton-ionizable lariat ethers - Effect of cavity size. *Sep. Purif. Technol.* **2006**, *48*, 264–269.

29 Bouchard, M.; Auger, M. Solvent history dependence of gramicidin-lipid interactions - a Raman and infrared spectroscopic study. *Biophys. J.* **1993**, *65*, 2484–2492.

30 Bechinger, B.; Salnikov, E. S. The membrane interactions of antimicrobial peptides revealed by solid-state NMR spectroscopy. *Chem. Phys. Lipids* **2012**, *165*, 282–301.

31 Ouellet, M.; Bernard, G.; Voyer, N.; Auger, M. Insights on the interactions of synthetic amphipathic peptides with model membranes as revealed by P-31 and H-2 solid-state NMR and infrared spectroscopies. *Biophys. J.* **2006**, *90*, 4071–4084.

32 Ouellet, M.; Voyer, N.; Auger, M. Membrane interactions and dynamics of a 21-mer cytotoxic peptide: A solid-state NMR study. *Biochim. Biophys. Acta, Biomembr.* **2010**, *1798*, 235–243.

33 Tansil, N. C.; Gao, Z. Q. Nanoparticles in biomolecular detection. *Nano Today* **2006**, *1*, 28–37.

34 Lu, F.; Doane, T. L.; Zhu, J. J.; Burda, C. Gold nanoparticles for diagnostic sensing and therapy. *Inorg. Chim. Acta* **2012**, *393*, 142–153.

35 Frasconi, M.; Mazzei, F.; Ferri, T. Protein immobilization at gold-thiol surfaces and potential for biosensing. *Anal. Bioanal. Chem.* **2010**, *398*, 1545–1564.

36 Wen, X. G.; Linton, R. W.; Formaggio, F.; Toniolo, C.; Samulski, E. T. Self-assembled monolayers of hexapeptides on gold: Surface characterization and orientation distribution analysis. *J. Phys. Chem. A* **2004**, *108*, 9673–9681.

37 Wilchek, M.; Bayer, E. A. Biotin-containing reagents. *Method. Enzymol.* **1990**, *184*, 123–138.

38 Voyer, N.; Arseneault, M.; Otis, F. Synthesis and characterization of peptide nanostructures designed for sensing applications. *Proc. SPIE Int. Soc. Opt. Eng.* **2005**, *5969*, 125–132.

39 Gorelik, E.; Galili, U.; Raz, A. On the role of cell surface carbohydrates and their binding proteins (lectins) in tumor metastasis. *Cancer Metastasis Rev.* **2001**, *20*, 245–277.

40 Boudreault, P. L.; Arseneault, M.; Otis, F.; Voyer, N. Nanoscale tools to selectively destroy cancer cells. *Chem. Commun.* **2008**, 2118–2120.